Scale properties of the seismic wavefield – perspectives for full waveform matching

GEOPHYSICS. VOL. 76, NO. 5 (SEPTEMBER-OCTOBER 2011); P. A37–A44, 4 FIGS., 3 TABLES.
10.1190/GEO2010-0213.1

# Scale properties of the seismic wavefield perspectives for full-waveform matching

Margherita Maraschini[1], Daniele Boiero[2], Sebastiano Foti[3], and Laura Valentina Socco[2]

## ABSTRACT

Starting from the nondimensionalization of equations of motion we partition the set of the velocity models in equivalence classes, such that the full waveform of an element in a given class can be calculated from the full waveform of any other element in the same class by scaling model parameters. We give a formal derivation of the seismic wavefield scale properties and we prove their capability through the use of numerical examples. Besides this, we introduce how the scale properties can be used to save computational time in full waveform modeling and inversion. In forward modeling we can use them for the calculation of the full waveform of any model in the same equivalence class of a model whose full waveform has been previously calculated. In full waveform inversion, scale properties can be used for full waveform matching: Given an experimental seismogram and a synthetic one, we can choose, in the same class of the synthetic model, another element whose waveform is closer to the experimental one.

## INTRODUCTION

Scale properties of seismic waves are relations between solutions of different seismic models whose parameters differ for scaling factors. Partitioning the set of seismic models in equivalence classes such that seismic parameters of two models in the same class differ for scaling factors, the ground displacement for a given model can be obtained from the ground displacement of any model in the same class if the source is appropriately scaled. Consequently, the Green's function of a model in a class can be calculated from the Green's function of another model in the same class by scaling the variables. Scale properties are based on equation nondimensionalization: If two models have the same nondimensional equations, the solution of the two problems is only scaled.

Scale properties (or equation nondimensionalization) are used in several technical and scientific fields. They can be used to improve algorithm convergence (Barral et al., 2004), to reduce the number of parameters (Galvanetto, 1999), to build small-scale physical models as in wind tunnel simulations (Corti et al., 2001), and in geotechnical centrifuge (Taylor, 1995; Zornberg et al., 1997). Besides this, scale properties allow simulation results to be generalized (Carr and Erneux, 2001; Amatore et al., 2007) and important nondimensional modeling parameters (e.g., Reynolds number) to be calculated (Boyer, 2002; Nika et al., 2005).

In geophysics, scale properties are implicitly used when a model is described in terms of parameter contrasts rather than parameter values. The normalization with respect to the wavelength, which is often applied in the description of seismic wave propagation, is a sort of scaling.

Concerning the surface wave propagation, scale properties of the dispersion curves, described by Socco and Strobbia (2004), have been formally demonstrated and applied in a Monte Carlo inversion by Socco and Boiero (2008). They propose a method to exploit scale properties: For each randomly sampled model, the dispersion curve is calculated and shifted close to the experimental curve. Scale factors, derived by the shift parameters, are then applied to the original model to improve the efficiency of the Monte Carlo inversion. A similar approach has been used by Piatti et al. (2010) for the inversion of vertical electrical sounding and time-domain electromagnetic data.

Here we present a formal demonstration of scale properties for wave propagation in elastic media. We show that "similar" seismic models (i.e., belonging to the same equivalence class) present "similar" displacement fields and "similar" Green's functions (i.e., they can be described by the same dimensionless equations for an ad hoc set of nondimensionalization factors or characteristic units).

Manuscript received by the Editor 16 July 2010; revised manuscript received 25 November 2010; published online 22 November 2011.
[1] Politecnico di Torino, DITAG, Italy, Currently at Fugro Seismic Imaging UK. E-mail: marghe.mar@gmail.com.
[2] Politecnico di Torino DITAG, Italy. E-mail: daniele.boiero@polito.it, valentina.socco@polito.it.
[3] Politecnico di Torino, DISTR, Italy. E-mail: sebastiano.foti@polito.it.

To prove this statement, we perform numerical simulations scaling the modeling variables and comparing the results. Through the use of the same synthetic seismograms, we show how scale properties may be applied to improve the efficiency of modeling and inversion.

In forward modeling, the full waveform of a specific model can be obtained scaling the full waveform of another model of the same class. In inversion, the scale properties can be used to reduce one or more units of the dimension of the model parameter space considered for the inversion. They can also be applied to efficiently reduce the misfit between the experimental and the synthetic seismogram, improving the performance of search algorithms.

## METHOD

### Equivalence classes

Let us call $S$ the set of all the ground seismic models. The set $S$ can be subdivided in equivalence classes $S_i$ by means of an equivalence relation: Two models A and B belong to the same equivalence class only if it is possible to find nondimensionalization factors (called characteristic units in the following) such that nondimensional equations of motion of the models (Appendix A) are the same.

The displacement field and the Green's function of B can be calculated from the displacement field and the Green's function of A by scaling the variables. Consequently, for each class, the forward operator needs to be calculated only once (Figure 1).

### Wave equation nondimensionalization

The demonstration of scale properties for an elastic model is based on the nondimensionalization of equations of motion, which is obtained by dividing all the quantities for characteristic units (Appendices A and B).

Let's consider two seismic models, A and B. The models A and B belong to the same class (i.e., they have the same equations of motion for ad hoc sets of characteristic units) only if there exist some constants $\alpha$, $\beta$, $\gamma$ such that:

$$V^2_{\mathrm{PB}}(\mathbf{x}) = \left(\frac{\alpha}{\beta}\right)^2 V^2_{\mathrm{PA}}\left(\frac{\mathbf{x}}{\alpha}\right),$$

$$V^2_{\mathrm{SB}}(\mathbf{x}) = \left(\frac{\alpha}{\beta}\right)^2 V^2_{\mathrm{SA}}\left(\frac{\mathbf{x}}{\alpha}\right),$$

$$\rho_{\mathrm{B}}(x) = \gamma \rho_{\mathrm{A}}\left(\frac{\mathbf{x}}{\alpha}\right), \tag{1}$$

$$\mathbf{f}_{\mathrm{B}}(\mathbf{x},t) = \gamma \frac{\alpha}{\beta^2}\mathbf{f}_{\mathrm{A}}\left(\frac{\mathbf{x}}{\alpha},\frac{t}{\beta}\right),$$

$$\mathbf{f}_{\mathrm{SB}}(\mathbf{x},t) = \gamma \left(\frac{\alpha}{\beta}\right)^2 \mathbf{f}_{\mathrm{SA}}\left(\frac{\mathbf{x}}{\alpha},\frac{t}{\beta}\right),$$

where $\mathbf{x}$ is the spatial coordinate, $t$ is the time, $V_{\mathrm{PA}}$ and $V_{\mathrm{PB}}$ are the P-wave velocities of models A and B, respectively, $V_{\mathrm{SA}}$ and $V_{\mathrm{SB}}$ are the S-wave velocities of models A and B, respectively, $\rho_{\mathrm{A}}$ and $\rho_{\mathrm{B}}$ are the densities of models A and B, respectively, $\mathbf{f}_A(\mathbf{x},t)$ and $\mathbf{f}_B(\mathbf{x},t)$ are the body force applied to the medium for $t > 0$ of models A and B, respectively, $\mathbf{f}_{\mathrm{SA}}(\mathbf{x},t)$ and $\mathbf{f}_{\mathrm{SB}}(\mathbf{x},t)$ are the pressure applied to the medium surface for $t > 0$ of models A and B, respectively, $\alpha$ is the ratio between lengths, $\beta$ is the ratio between times, and $\gamma$ is the ratio between densities. In the following $\alpha$, $\beta$, and $\gamma$ are called scale factors.

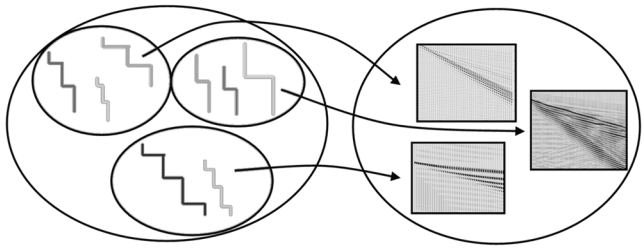

Figure 1. Schematization of the partition of all possible models in equivalence classes.

When sources are appropriately scaled, the displacements of model B can be calculated from displacements of model A as

$$\mathbf{u}_B(\mathbf{x},t) = \alpha \mathbf{u}_A\left(\frac{\mathbf{x}}{\alpha},\frac{t}{\beta}\right), \tag{2}$$

and the Green's functions $\mathbf{G}_n(\mathbf{x},t;\xi,\tau)$ of the two profiles are related by the analytical relation (see Appendix C and equation C-4):

$$\mathbf{G}_{nB}(\mathbf{x},t;\xi,\tau) = \frac{\beta}{\alpha^3\gamma}\mathbf{G}_{nA}\left(\frac{\mathbf{x}}{\alpha},\frac{t}{\beta};\frac{\xi}{\alpha},\frac{\tau}{\beta}\right), \tag{3}$$

where $\mathbf{u} = \mathbf{u}(\mathbf{x},t)$ is the displacement vector, $\mathbf{G}_n = \mathbf{G}_n(\mathbf{x},t;\boldsymbol{\xi},\tau)$ is the displacement Green's function generated by an impulsive source in direction $n$ applied in $\mathbf{x} = \boldsymbol{\xi}$ and $t = \tau$.

## APPLICATIONS

### Example of full-waveform modeling

We generated two synthetic seismograms through a finite element method code (Comsol Multiphysics®) using an axial symmetric scheme and a Ricker wavelet source (the same in the two models). The models (in the following A and B) are 1D linear elastic isotropic, and the model parameters are summarized in Table 1. The two models belong to the same equivalence class, and the scale factors are: $\alpha = 2$, $\beta = 1.25$, $\gamma = 1.11$. The sensor's spacing, according to $\alpha$, is 4 m for model A, and 8 m for model B, while the sampling rate, according to $\beta$, is 1 ms for model A, and 1.25 ms for model B.

The seismograms of models *A* and *B* are shown in Figure 2a and Figure 2b, respectively. The two seismograms differ for offsets and times, which are scaled by $\alpha$ and $\beta$, respectively (Figure 2c). Comparing the displacements for each trace of the seismogram *A* with the corresponding displacements of the seismogram *B*, we observe that the shape is the same, while the amplitudes are scaled (Figure 2d). In this specific case, since the sources on the surface ($\mathbf{f}_{SA}$ and $\mathbf{f}_{SB}$) are equal in amplitude, the displacements are scaled by a factor $\delta(\alpha,\beta,\gamma)$ that can be derived by taking into account the source and the displacement scaling (equations 1 and 2), and it can be calculated as:

**Table 1. Characteristics of 1D seismic models A and B.**

| Layer | $h_A$ (m) | $V_{SA}$ (m/s) | $V_{PA}$ (m/s) | $\rho_A$ (kg/m$^3$) | $h_B$ (m) | $V_{SB}$ (m/s) | $V_{PB}$ (m/s) | $\rho_B$ (kg/m$^3$) |
|---|---|---|---|---|---|---|---|---|
| 1 | 5 | 90 | 180 | 1800 | 10 | 144 | 288 | 2000 |
| 2 | 10 | 140 | 280 | 1800 | 20 | 224 | 448 | 2000 |
| 3 | — | 200 | 400 | 1800 | — | 320 | 640 | 2000 |

$$\delta = \frac{\alpha^3 \gamma}{\beta^2}, \tag{4}$$

where $\alpha$, $\beta$, and $\gamma$ are the scale factors defined above.

For this example, according to equation 4, $\delta$ is equal to 5.69, and it is the ratio between the displacements of A and B (Figure 2e).

The full waveform for model *B* could have been directly obtained from the one computed for model *A* just scaling offsets, times, and amplitudes of traces according to the scale factors between the two models. With the same procedure, synthetic seismograms can be evaluated for every model belonging to the class of A and B.

## Example of full-waveform matching

To show the perspective of the scale properties in full waveform matching, we consider two models A and C (Table 2) belonging to different equivalence classes, and we show how the scale properties can be used to efficiently improve the full waveform matching between them. This can be done in analogy with the approach proposed by Socco and Boiero (2008) in surface wave inversion of dispersion curves. In that case, they used ratios between the barycenter coordinates of two dispersion curves (in the frequency-velocity domain) to retrieve scaling factors. The idea was to identify a point, which was representative of the dispersion curves, in order to evaluate scaling factors to be applied to subsoil models that make the dispersion curves get closer (without evaluating the forward problem).

With this aim, for the rastered image of each seismogram (Figure 3a and Figure 3b), we evaluate the image barycenter position (identified by black stars). The barycenter coordinates are reported in Table 3 for models A and C respectively and their ratios allow the scaling factors ($\alpha = 1.75$, $\beta = 1.28$) to be calculated (Table 3). In Figure 3c, we show the rastered image of the seismogram obtained from model C after the scaling. The retrieved scaling factors can be applied to the *S*- and *P*-wave velocity functions characterizing the model C (Figure 3d) to reduce their difference with respect to the velocity functions characterizing the model A (Figure 3e). The

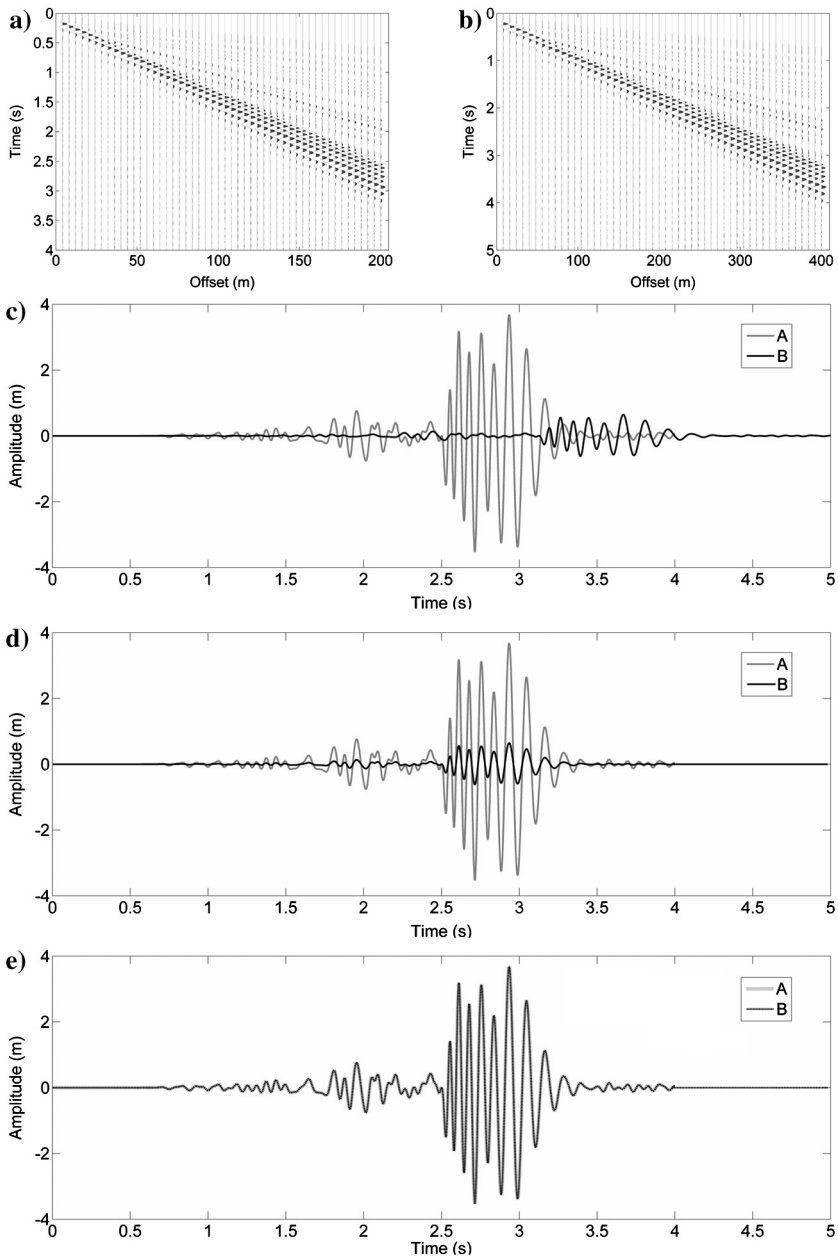


Figure 2. (a) Synthetic seismograms (normalized) model A; (b) Synthetic seismograms (normalized) model B; (c) comparison of the displacements: trace at offset 200 m for model A (solid gray); trace at offset 400 m for model B (solid black); (d) comparison of displacements: trace at offset 200 m for model A (solid gray); trace at offset 400 m for model B with time scaled by 1.25 (solid black); (d) comparison of displacements: trace at offset 200 m for model A (solid gray); trace at offset 400 m for model B with time and amplitude scaled by 1.25 and 5.69 respectively (black dots).

same reduction can be observed in the full waveform matching between the two seismograms comparing the ground displacements at 104 m in offset (Figure 4a), and at 1 s in time (Figure 4b). The displacements for model C are stretched in time and space and scaled in amplitude (by a factor $\beta^2/\alpha^3$), to become more similar to the displacements for model A.

The full waveform matching can be further improved by considering the scale factor $\gamma$ (Figure 4a and Figure 4b). After estimating $\alpha$ and $\beta$, from the ratio between the averages of the absolute amplitude values of the displacements for A and C (Table 4) we also can estimate $\delta(\alpha, \beta, \gamma)$ (equation 4) and consequently evaluate the contribute of $\gamma = 1.06$.

From the example above, if the two models do not belong to the same class, the application of the scale properties and the retrieved scaling factors does not provide a perfect match of the two seismograms, but allows the distance between the two models to be reduced. Hence, scale properties could represent a tool for full waveform inversion.

**Table 2. Characteristics of 1D seismic models A and C.**

| Layer | $h_A$ (m) | $V_{SA}$ (m/s) | $V_{PA}$ (m/s) | $\rho_A$ (kg/m$^3$) | $h_C$ (m) | $V_{SC}$ (m/s) | $V_{PC}$ (m/s) | $\rho_C$ (kg/m$^3$) |
|---|---|---|---|---|---|---|---|---|
| 1 | 5 | 90 | 180 | 1800 | 9 | 130 | 300 | 2000 |
| 2 | 10 | 140 | 280 | 1800 | 23 | 240 | 460 | 2000 |
| 3 | — | 200 | 400 | 1800 | — | 310 | 620 | 2000 |

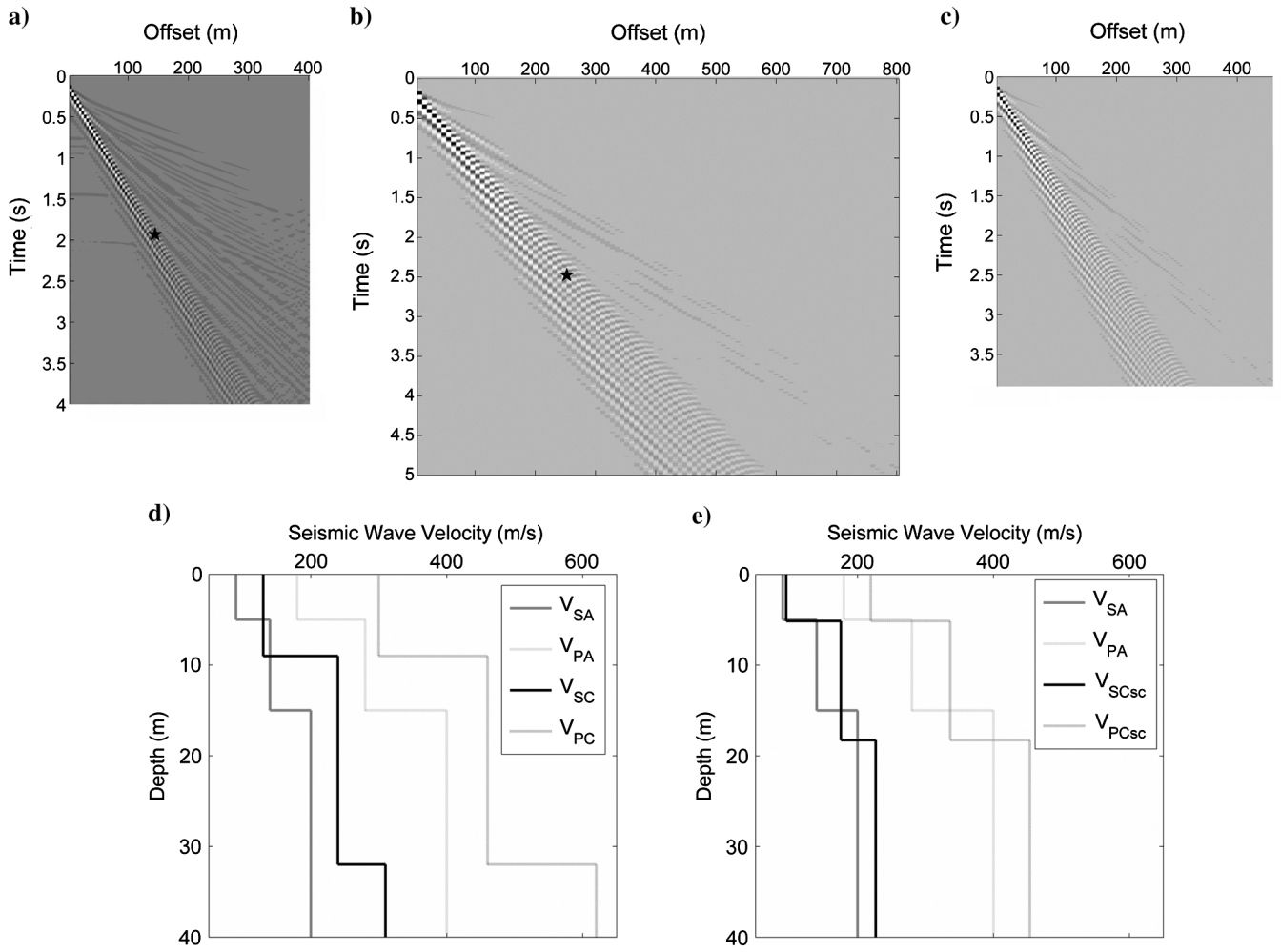


Figure 3. (a) rastered synthetic seismogram for model A with the barycenter (black star); (b) rastered synthetic seismogram for model C with the barycenter (black star); (c) rastered synthetic seismogram for model C after scaling; (d) S-wave ($V_S$) and P-wave ($V_P$) velocity function of model A (solid gray and gray dots respectively) and C (solid black and black dots respectively); (e) S-wave ($V_S$) and P-wave ($V_P$) velocity function of model A (solid gray and gray dots respectively) and C (solid black and black dots respectively) after scaling.

**Table 3. Estimation of the scaling factors between A and C.**

| Model | A | C | Ratio C/A |
|---|---|---|---|
| Barycenter offset (m) | 144.6 | 252.4 | $\alpha = 1.75$ |
| Barycenter time (s) | 1.935 | 2.478 | $\beta = 1.28$ |
| Average amplitude (m) | \|3.135\| | \|0.904\| | $\delta = 3.47$ |

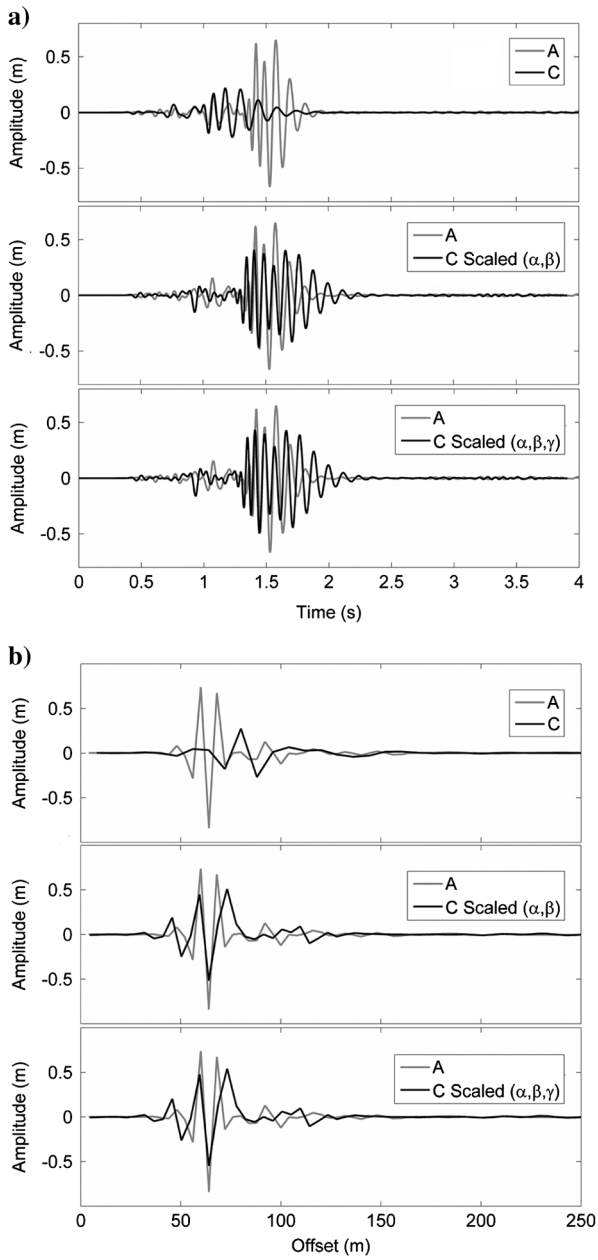


Figure 4. (a) displacements of model A (solid gray) and C (solid black) at offset 104 m. The model C is scaled applying the scale factors $\alpha$, $\beta$ and $\gamma$ at different stages; (b) displacements of model A (solid gray) and displacements of model C (solid black) at time 1 s. The model C is scaled applying the scale factors $\alpha$, $\beta$ and $\gamma$ at different stages.

## DISCUSSION

Considering a seismic model as representative of an equivalence class of models allows the seismogram relative to the considered model to be associated to any model of that class after proper scaling. We demonstrate this in the example reported in Figure 2, where the seismogram of one model is obtained by the application of proper scale factors from the seismogram of another model of the same equivalence class. In this way, instead of considering each model to be unique, we can consider model classes. Model space can be thus represented in a more efficient way through model classes, and each model class can be described by a representative model from which all the others can be directly derived. This can be profitably exploited in inversion, especially for global search methods (as shown by Socco and Boiero (2008) for the case of surface wave dispersion curves) or for full-waveform inversions, which are computationally expensive. In particular, the spatial and temporal scaling aspects of the method make it useful to efficiently estimate the background velocity (Figure 3d and 3e).

We consider the example presented in Figures 3 and 4, and assume that the seismogram of model A is real data to be inverted. If model C is a randomly generated model in a global search inversion, or an initial model for a linearized inversion, instead of comparing the synthetic seismogram relative to C with the real data (A) in a misfit function, we can (1) compare the two seismograms and retrieve the model scale factors, (2) update the model C according to this scale factors, and (3) compute the misfit between the real data and the scaled seismogram. In this way, starting from an initial (or random-generated) model which is quite far from the true one, we can move closer to the true model by reducing the misfit between the data, and without the need of computing again the forward model. What we do is, instead of considering a generic model of a class and comparing it to our data, we move to the model, in the same class of the generic one, which is the closest (or at least closer) to the true one. This means that, instead of performing a random sampling of model space, we could perform a random sampling among model classes, thus reducing the number of required forward model calculations in a global search approach (Socco and Boiero, 2008; Piatti et al., 2010).

Another possible application, which is not an object of this paper, could be the comparison of different field data to retrieve the scaling factors between different locations at a site.

## CONCLUSIONS

Scale properties of seismic waves can be used to save computation time in full waveform modeling and inversion of elastic seismic models. The nondimensionalization of equations of motion allows the possible models to be divided into classes, such that the full waveform of one of the elements in a class can be directly calculated from the full waveform of another element in the same class by applying the scale factors between the two models.

Two main applications are presented. In forward modeling, if the full waveform is simulated for a given model, it is straightforward to get the full waveform for any other model in the same class. In full waveform matching, when an experimental seismogram is recorded and a synthetic one is calculated, it can be useful to retrieve the scale factors between experimental and synthetic data, and consequently update the synthetic model to another in the same class which is closer to the experimental one.

## ACKNOWLEDGMENTS

We thank Davide Ambrosi for valuable discussions and for offering us a different point of view on the subject.

We thank Kees Wapenaar for his helpful remarks on a preliminary version of this manuscript and for his useful comments during review, and two anonymous reviewers for their constructive remarks.

## APPENDIX A

## DERIVATION OF DIMENSIONLESS EQUATIONS FOR AN ELASTIC MODE

In this appendix, a formal derivation of dimensionless equations of motion is provided. The derivation can be subdivided in several steps:

- Choice of the model: Dimensional equations of motion can be written (equations A-1).
- Definition of characteristic units: Dimensional equations of motion are written replacing each dimensional variable with the product of a dimensionless variable and a dimensional characteristic unit (equations A-2).
- Equation adimensionalization: Characteristic units in the equations are used to define dimensionless parameters and forces (equations A-3). Each member of equations A-1 becomes dimensionless (equations A-4).
- The relation between the dimensional and dimensionless displacements is derived (equations A-5).

The demonstration is given for an isotropic medium, but the generalization to a nonisotropic medium only increments the number of model parameters that must be opportunely scaled.

The equations of motion for a heterogeneous half-space are (Aki and Richards, 1980):

$$\begin{cases} \rho(\mathbf{x})\dfrac{\partial^2\mathbf{u}}{\partial t^2} = \mathbf{f}(\mathbf{x},t) \\ \qquad + [(\lambda(\mathbf{x})+\mu(\mathbf{x}))\nabla\nabla\cdot\mathbf{u} + \mu(\mathbf{x})\Delta\mathbf{u}], & t \geq 0, x_3 > 0, \\ (\sigma\mathbf{n}) = [(\mu(\mathbf{x})(\nabla\mathbf{u} + \nabla\mathbf{u}^T) \\ \qquad + \lambda(\mathbf{x})\nabla\cdot\mathbf{u}I)(0,0,1)^T] = \mathbf{f_S}(\mathbf{x},t), & t \geq 0, x_3 = 0, \\ \mathbf{u} \to \mathbf{0}, & t \geq 0, \|\mathbf{x}\| \to \infty, \\ \mathbf{u} = \mathbf{0}, & t < 0, \\ \dfrac{\partial\mathbf{u}}{\partial t} = \mathbf{0}, & t < 0, \end{cases} \tag{A-1}$$

where:

$\mathbf{u} = \mathbf{u}(\mathbf{x},t)$ is the vector of the displacement;
$\mathbf{f}(\mathbf{x},t)$ is the body force applied to the medium for $t > 0$;
$\mathbf{f_S}(\mathbf{x},t)$ is the pressure applied to the medium surface for $t > 0$;
$x_3$ is the vertical direction oriented downward;
$I$ is the unit matrix;
$T$ represents the transpose of a given matrix;
$\sigma\mathbf{n}$ is the stress vector applied to the interface between adjacent layers;
$\lambda$ and $\mu$ are the Lamé's constants;
$\rho$ is the density of the medium;
$\nabla$, $\nabla\cdot$, $\Delta$ represent the gradient operator, the divergence operator, and the Laplacian operator, respectively.

These equations can be nondimensionalized dividing all the quantities for the nondimensionalization factors, and changing the variables. We can write:

$$\mathbf{x} = \hat{L}\mathbf{X}, \quad \mathbf{u}(\mathbf{x},t) = \hat{L}\mathbf{U}(\mathbf{X},T), \quad \rho = \hat{R}R,$$
$$t = \hat{T}T, \quad v = \frac{\hat{L}}{\hat{T}}V; \tag{A-2}$$

where $v$ is the seismic velocity, small letters represent dimensional variables, capital letters represent dimensionless variables and capital letters with hat represent the characteristic units. Moreover in the following $\hat{\Delta}$, $\hat{\nabla}$, $\hat{\nabla}\cdot$ represent the differential operators with respect to the nondimensional variables.

Using characteristic units in equations A-2, we define, for a generic model, nondimensional P-wave velocity $V_P$, and S-wave velocity $V_S$, density and nondimensional volume and surface forces as:

$$\begin{aligned} V_P^2(\mathbf{X}) &= \frac{\hat{T}^2}{\hat{L}^2}\frac{\lambda(\hat{L}\mathbf{X}) + 2\mu(\hat{L}\mathbf{X})}{\rho(\hat{L}\mathbf{X})} = \frac{\hat{T}^2}{\hat{L}^2}v_P^2(\hat{L}\mathbf{X}), \\ V_S^2(\mathbf{X}) &= \frac{\hat{T}^2}{\hat{L}^2}\frac{\mu(\hat{L}\mathbf{X})}{\rho(\hat{L}\mathbf{X})} = \frac{\hat{T}^2}{\hat{L}^2}v_S^2(\hat{L}\mathbf{X}), \\ R(\mathbf{X}) &= \frac{\rho(\hat{L}\mathbf{X})}{\hat{R}}, \\ \mathbf{F}(\mathbf{X},T) &= \frac{\hat{T}^2}{\hat{L}\hat{R}}\mathbf{f}(\hat{L}\mathbf{X},\hat{T}T), \\ \mathbf{F}_S(\mathbf{X},T) &= \frac{\hat{T}^2}{\hat{L}^2\hat{R}}\mathbf{f}_S(\hat{L}\mathbf{X},\hat{T}T). \end{aligned} \tag{A-3}$$

According to equations A-3, equations A-1 can be written as:

$$\begin{cases} \dfrac{\partial^2\mathbf{U}}{\partial T^2} = \dfrac{1}{R(\mathbf{X})}\mathbf{F}(\mathbf{X},T) \\ \qquad + [(V_P^2(\mathbf{X}) - V_S^2(\mathbf{X}))\hat{\nabla}\hat{\nabla}\cdot\mathbf{U} + V_S^2(\mathbf{X})\hat{\Delta}\mathbf{U}], & TT \geq 0, X_3 > 0, \\ \{[V_S^2(\mathbf{X})R(\mathbf{X})(\hat{\nabla}\mathbf{U} + \hat{\nabla}\mathbf{U}^T) \\ +(V_P^2(\mathbf{X}) - 2V_S^2(\mathbf{X}))R(\mathbf{X})\hat{\nabla}\cdot\mathbf{U}I](0,0,1)^T\} = \\ = \mathbf{F}_S(\mathbf{X},T) & T \geq 0, X_3 > 0, \\ \mathbf{U} \to \mathbf{0}, & T \geq 0, \|\mathbf{X}\| \to \infty, \\ \mathbf{U} = \mathbf{0}, & T \leq 0, \\ \dfrac{\partial\mathbf{U}}{\partial T} = \mathbf{0}, & T \leq 0. \end{cases} \tag{A-4}$$

All the quantities present in equations A-4 are dimensionless. The solution of the system does not depend on model parameters, but on the ratio between model parameters and their characteristic units.

If $\mathbf{U}(\mathbf{X},T)$ is the solution of the dimensionless equations A-4, the solution of equations A-1 is:

$$\mathbf{u}(\mathbf{x},t)=\hat{L}\mathbf{U}\left(\frac{\mathbf{x}}{\hat{L}},\frac{t}{\hat{T}}\right). \tag{A-5}$$

Two models which, for an ad hoc set of model parameters, present the same dimensionless equations A-4 (i.e., belong to the same equivalence class) have the same dimensionless wavefield, and the dimensional wavefield of a model can be calculated from the dimensional wavefield of the other one through the dimensionless wavefield.

## APPENDIX B

## SCALE PROPERTIES FOR TWO ELASTIC MODELS BELONGING TO THE SAME EQUIVALENCE CLASS

In this appendix, we show that two elastic models whose parameters and forces are proportional belong to the same class.

To demonstrate this we start from:

- models A and B belong to the same class, only if we can define characteristic units (equations A-2) such that the dimensionless equations of the two models are the same.
- dimensionless equations A-4 for the two models coincide only if dimensionless parameters defined in equations A-3 coincide, or with simple math, if:

$$\begin{aligned}
v_{PB}^2(\hat{L}_B\mathbf{X})&=\left(\frac{\hat{L}_B}{\hat{L}_A}\frac{\hat{T}_A}{\hat{T}_B}\right)^2 v_{PA}^2(\hat{L}_A\mathbf{X})=\\
&=\left(\frac{\alpha}{\beta}\right)^2 v_{PA}^2(\hat{L}_A\mathbf{X}),\\
v_{SB}^2(\hat{L}_B\mathbf{X})&=\left(\frac{\hat{L}_B}{\hat{L}_A}\frac{\hat{T}_A}{\hat{T}_B}\right)^2 v_{SA}^2(\hat{L}_A\mathbf{X})=\\
&=\left(\frac{\alpha}{\beta}\right)^2 v_{SA}^2(\hat{L}_A\mathbf{X}),\\
\rho_B(\hat{L}_B\mathbf{X})&=\frac{\hat{R}_B}{\hat{R}_A}\rho_A(\hat{L}_A\mathbf{X})=\gamma\rho_A(\hat{L}_A\mathbf{X}),\\
\mathbf{f}_B(\hat{L}_B\mathbf{X},\hat{T}T)&=\frac{\hat{T}_A{}^2\hat{L}_B\hat{R}_B}{\hat{T}_B{}^2\hat{L}_A\hat{R}_A}\mathbf{f}_A(\hat{L}_A\mathbf{X},\hat{T}T)=\\
&=\gamma\frac{\alpha}{\beta^2}\mathbf{f}_A(\hat{L}_A\mathbf{X},\hat{T}T),\\
\mathbf{f}_{SB}(\hat{L}_B\mathbf{X},\hat{T}T)&=\frac{\hat{T}_A{}^2\hat{L}_A{}^2\hat{R}_B}{\hat{T}_B{}^2\hat{L}_A{}^2\hat{R}_A}\mathbf{f}_{SA}(\hat{L}_A\mathbf{X},\hat{T}T)=\\
&=\gamma\left(\frac{\alpha}{\beta}\right)^2\mathbf{f}_{SA}(\hat{L}_A\mathbf{X},\hat{T}T),
\end{aligned} \tag{B-1}$$

where $\alpha=\hat{L}_B/\hat{L}_A$, $\beta=\hat{T}_B/\hat{T}_A$, $\gamma=\hat{R}_B/\hat{R}_A$.

Equations B-1 imply equations 1. Free surface conditions of nondimensional equations are automatically coincident if equations 1 are verified, i.e., if and only if the two models belong to the same class.

When two models belong to the same class, the relation between displacements of model B from displacements of model A can be obtained from equation A-5, remembering that the dimensionless solution $\mathbf{U}=\mathbf{U}_A=\mathbf{U}_B$ is the same for the two models:

$$\begin{aligned}
\mathbf{u}_B(\mathbf{x},t)&=\hat{L}_B\mathbf{U}\left(\frac{\mathbf{x}}{\hat{L}_B},\frac{t}{\hat{T}_B}\right)=\\
&=\frac{\hat{L}_B}{\hat{L}_A}\mathbf{u}_A\left(\frac{\mathbf{x}}{\hat{L}_B}\hat{L}_A,\frac{t}{\hat{T}_B}\hat{T}_A\right)=\\
&=\alpha\mathbf{u}_A\left(\frac{\mathbf{x}}{\alpha},\frac{t}{\beta}\right).
\end{aligned} \tag{B-2}$$

## APPENDIX C

## SCALE PROPERTIES OF GREEN'S FUNCTIONS FOR TWO ELASTIC MODELS BELONGING TO THE SAME EQUIVALENCE CLASS

When two models A and B belong to the same equivalence class, it is possible to calculate the Green's function of model B starting from the Green's function of model A.

In order to calculate the relation between the Green's functions for the two models, let us define:

$$\begin{aligned}
\mathbf{f}_A(\mathbf{x},t)&=\delta(\mathbf{x}-\xi)\delta(t-\tau);\\
\mathbf{f}_{SA}(\mathbf{x},t)&=\left[\int_{-\infty}^{\infty}\delta(\mathbf{x}-\xi)\mathrm{d}x_3\right]\delta(t-\tau),
\end{aligned} \tag{C-1}$$

where $\delta(\mathbf{x}-\xi)$ is a 3D Dirac delta function, i.e., a function defined on $R^3$ which is 0 if $\mathbf{x}\neq\xi$ and such that $\int_{-\infty}^{\infty}\int_{-\infty}^{\infty}\int_{-\infty}^{\infty}\delta(\mathbf{x}-\xi)\mathrm{d}x_1\mathrm{d}x_2\mathrm{d}x_3=1$. Consequently $\int_{-\infty}^{\infty}\delta(\mathbf{x}-\xi)\mathrm{d}x_3$ is a 2D Dirac delta function, defined on $R^2$.

From equations 1, the corresponding volume and surface forces for model B are:

$$\begin{aligned}
\mathbf{f}_B(\mathbf{x},t)&=\gamma\frac{\alpha}{\beta^2}\delta\left(\frac{\mathbf{x}-\xi}{\alpha}\right)\delta\left(\frac{t-\tau}{\beta}\right),\\
\mathbf{f}_{SB}(\mathbf{x},t)&=\gamma\left(\frac{\alpha}{\beta}\right)^2\left[\int_{-\infty}^{\infty}\delta\left(\frac{\mathbf{x}-\xi}{\alpha}\right)\mathrm{d}\frac{x_3}{\alpha}\right]\delta\left(\frac{t-\tau}{\beta}\right),
\end{aligned} \tag{C-2}$$

which are scaled delta distribution. Their integrals are respectively:

$$\begin{aligned}
&\int_{\mathbf{x},t}\mathbf{f}_B(\mathbf{x},t)dx_1dx_2dx_3dt=\\
&\quad=\int_{\mathbf{x},t}\gamma\frac{\alpha}{\beta^2}\delta\left(\frac{\mathbf{x}-\xi}{\alpha}\right)\delta\left(\frac{t-\tau}{\beta}\right)dx_1dx_2dx_3dt=\\
&\quad=\gamma\frac{\alpha^4}{\beta}\int_{\mathbf{x},t}\delta\left(\frac{\mathbf{x}-\xi}{\alpha}\right)\delta\left(\frac{t-\tau}{\beta}\right)d\frac{x_1}{\alpha}d\frac{x_2}{\alpha}d\frac{x_3}{\alpha}d\frac{t}{\beta}=\gamma\frac{\alpha^4}{\beta},
\end{aligned}$$

and

$$\begin{aligned}
&\int_{x_1,x_2,t}\mathbf{f}_{SB}(\mathbf{x},t)dx_1dx_2dt=\\
&\quad=\int_{x_1,x_2,t}\gamma\left(\frac{\alpha}{\beta}\right)^2\left[\int_{-\infty}^{\infty}\delta\left(\frac{\mathbf{x}-\xi}{\alpha}\right)\mathrm{d}\frac{x_3}{\alpha}\right]\delta\left(\frac{t-\tau}{\beta}\right)dx_1dx_2dt=\\
&\quad=\gamma\frac{\alpha^4}{\beta}\int_{\mathbf{x},t}\delta\left(\frac{\mathbf{x}-\xi}{\alpha}\right)\delta\left(\frac{t-\tau}{\beta}\right)d\frac{x_1}{\alpha}d\frac{x_2}{\alpha}d\frac{t}{\beta}=\gamma\frac{\alpha^4}{\beta}.
\end{aligned} \tag{C-3}$$

Calling $\mathbf{G}_{nA} = \mathbf{G}_{nA}(x,t;\xi,\tau) = \mathbf{u}_{\mathrm{A}}(\mathbf{x},t)$ the Green's function generated by an impulsive source in direction $n$ applied at $\mathbf{x} = \xi$ and $t = \tau$ for model A, from equation B-2 and equations C-3, we can write:

$$\begin{aligned}\mathbf{G}_{nB}(\mathbf{x},t;\xi,\tau) &= \frac{\beta}{\alpha^4\gamma}\mathbf{u}_B(\mathbf{x},t) = \\ &= \alpha\frac{\beta}{\alpha^4\gamma}\mathbf{u}_A\left(\frac{\mathbf{x}}{\alpha},\frac{t}{\beta}\right) = \\ &= \frac{\beta}{\alpha^3\gamma}\mathbf{G}_{nA}\left(\frac{\mathbf{x}}{\alpha},\frac{t}{\beta};\frac{\xi}{\alpha},\frac{\tau}{\beta}\right), \qquad \text{(C-4)}\end{aligned}$$

which is the relation between the Green's functions of the two models.

## REFERENCES


Aki, K., and P. G. Richards, 1980, Quantitative seismology: Theory and methods: Vol. **2**, Freeman.

Amatore, C., K. Knoblocha, and L. Thouin, 2007, Alteration of diffusional transport by migration and natural convection: Theoretical and direct experimental evidences upon monitoring steady-state concentration models at planar electrodes: Journal of Electroanalytical Chemistry, **601**, 17–28, doi: 10.1016/j.jelechem.2006.10.020.

Barral, P., C. Moreno, P. Quintela, and M. T. Sanchez, 2004, A numerical algorithm for a Signorini problem associated with Maxwell—Norton materials by using generalized Newton's methods: Computer Methods in Applied Mechanics and Engineering, **195**, no. 9-12, 880–904.

Boyer, F., 2002, A theoretical and numerical model for the study of incompressible mixture flows: Computers & Fluids, **31**, no. 1, 41–68.

Carr, T. W., and T. Erneux, 2001, Non-dimensional rate equations and simple conditions for self-pulsing in laser diodes: Journal of Quantum electronics, **37**, no. 9, 1171–1177.

Corti, A., M. Zanobini, and E. Canepa, 2001, Use of wind tunnel measurements for mathematical model comparison and validation: Proceedings, Second Conference on Air Pollution Modeling and Simulation, APMS'01, Champs-sur-Marne, April 9–12.

Galvanetto, U., 1999, Non-linear dynamics of multiple friction oscillators: Computer Methods in Applied Mechanics and Engineering, **178**, no. 3-4, 291–306, doi: 10.1016/S0045-7825(99)00021-3.

Nika, P., Y. Bailly, and F. Lanzetta, 2005, Heat transfer during incompressible oscillating laminar flow: International Journal of Refrigeration, **28**, no. 3, 353–367, doi: 10.1016/j.ijrefrig.2004.08.012.

Piatti, C., D. Boiero, A. Godio, and L. V. Socco, 2010, Improved Monte Carlo 1D inversion of vertical electrical sounding and time-domain electromagnetic data: Near Surface Geophysics, **8**, 117–133.

Socco, L. V., and D. Boiero, 2008, Improved Monte Carlo inversion of surface wave data: Geophysical Prospecting, **56**, 357–371, doi: 10.1111/j.1365-2478.2007.00678.x.

Socco, L. V., and C. Strobbia, 2004, Surface wave methods for near-surface characterisation, a tutorial: Near Surface Geophysics, **2**, 165–185.

Taylor, R. N., ed. 1995, Geotechnical centrifuge technology: Taylor & Francis, 296.

Zornberg, J. G., J. K. Mitchell, and N. Sitar, 1997, Testing of reinforced slopes in a geotechnical centrifuge: Geotechnical Testing Journal, **20**, no. 4, 470–480, doi: 10.1520/GTJ10413J.